Published in final edited form as:
J Ultrasound Med. 2011 March ; 30(3): 333–345.

Contrast-Enhanced Sonography Depicts Spontaneous Ovarian Cancer at Early Stages in a Preclinical Animal Model

Animesh Barua, PhD, **Pincas Bitterman, MD**, **Janice M. Bahr, PhD**, **Sanjib Basu, PhD**, **Eyal Sheiner, MD**, **Michael J. Bradaric, BS**, **Dale B. Hales, PhD**, **Judith L. Luborsky, PhD**, and **Jacques S. Abramowicz, MD**

Departments of Pharmacology (A.B., M.J.B., J.L.L.), Obstetrics and Gynecology (A.B., J.L.L., J.S.A.), Pathology (A.B., P.B.), and Preventive Medicine (S.B.), Rush University Medical Center, Chicago, Illinois; Department of Animal Sciences, University of Illinois at Urbana-Champaign, Urbana, Illinois (J.M.B.); Department of Physiology, Southern Illinois University, Carbondale, Illinois, USA (D.B.H.); and Department of Obstetrics and Gynecology, Soroka University Medical Center, Be'er Sheva, Israel (E.S.)

Abstract

Objective—Our goal was to examine the feasibility of using laying hens, a preclinical model of human spontaneous ovarian cancer, in determining the kinetics of an ultrasound contrast agent indicative of ovarian tumor-associated neoangiogenesis in early-stage ovarian cancer.

Methods—Three-year-old White Leghorn laying hens with decreased ovarian function were scanned before and after intravenous injection of a human serum albumin–perflutren contrast agent at a dose of 5 μL/kg body weight. Gray scale morphologic characteristics, Doppler indices, the arrival time, peak intensity, and wash-out of the contrast agent were recorded and archived on still images and video clips. Hens were euthanized thereafter; sonographic predictions were compared at gross examination; and ovarian tissues were collected. Archived clips were analyzed to determine contrast parameters and Doppler intensities of vessels. A time-intensity curve per hen was drawn, and the area under the curve was derived. Tumor types and the density of ovarian microvessels were determined by histologic examination and immunohistochemistry and compared to sonographic predictions.

Results—The contrast agent significantly ($P < .05$) enhanced the visualization of microvessels, which was confirmed by immunohistochemistry. Contrast parameters, including the time of wash-out and area under the curve, were significantly different ($P < .05$) between ovaries of normal hens and hens with ovarian cancer and correctly detected cancer at earlier stages than the time of peak intensity.

Conclusions—The laying hen may be a useful animal model for determining ovarian tumor-associated vascular kinetics diagnostic of early-stage ovarian cancer using a contrast agent. This model may also be useful for testing the efficacy of different contrast agents in a preclinical setting.

Keywords

contrast-enhanced sonography; early detection; ovarian cancer; ovarian tumor-associated neoangiogenesis; spontaneous animal model

Address correspondence to Animesh Barua, PhD, Laboratory for Translational Research on Ovarian Cancer, Departments of Pharmacology, Obstetrics and Gynecology, and Pathology, Rush University Medical Center, 1735 W Harrison St, Cohn Building, Room 456, Chicago IL 60612 USA. Animesh_Barua@rush.edu.

Neovascularization, preceded by malignant cellular transformation, is an early event during tumor development.[1,2] Tumor-associated neoangiogenesis has been shown to be a critical requirement for the progression and metastasis of malignant tumors of the ovary as well as other organs.[1,3,4] Therefore, ovarian tumor-associated neoangiogenesis represents the potential to be an early detection target for ovarian cancer, a fatal disease responsible for the highest death rate of women from all gynecologic malignancies.[5] Previous reports on the immunohistochemical localization of tumor microvessels in postoperative specimens have shown a positive relationship between tumor progression and tumor-associated neoangiogenesis and suggested the utility of ovarian tumor-associated neoangiogenesis as a tool for the detection of ovarian cancer at an early stage.[6–8] Therefore, an in vivo noninvasive method of detecting ovarian tumor-associated neoangiogenesis relative to early-stage ovarian cancer is highly desirable.

Gray scale and Doppler sonography are the noninvasive and currently recommended modalities for the evaluation of gynecologic abnormalities, including ovarian tumors. Although Doppler sonography can depict large intratumoral blood vessels, in many cases, including early-stage ovarian cancer, it cannot depict smaller neoangiogenic vessels.[9,10] Failure to distinguish benign from malignant ovarian tumors and to detect ovarian cancer at an early stage are the two main limitations of current Doppler sonography.[11,12] This failure of detection is either because the tumor-associated microvessels are too small or the Doppler shifts in these vessels are too weak to be detected by the current detection limits of ultrasound scanners.[13] Therefore, Doppler sonography may be an effective method for early detection of ovarian cancer if its current detection limit can be improved to depict ovarian tumor-associated neoangiogenesis. A moderate number of studies have shown the efficacy of ultrasound contrast agents for enhancing the sensitivity of traditional Doppler sonography to visualize blood vessels and distinguish malignant tumors from benign ones on the basis of intratumoral microvascular architecture.[13–16] There is limited literature evaluating contrast enhancement in adenexal masses, and, to our knowledge, most of the reported studies on ovarian imaging by contrast-enhanced sonography were based on patients with late-stage ovarian cancer because of the possible difficulty of obtaining access to patients with early-stage ovarian cancer.[13,14,17,18] Thus, observations on contrast-enhanced sonography in these studies may not be useful as such for early detection of ovarian cancer. Because the 5-year survival rates for patients with ovarian cancer are remarkably high when the disease is detected at an early stage, studies on contrast-enhanced sonography of early-stage ovarian cancer cases are needed to establish an early detection method for ovarian cancer.

Animal models serve as surrogates to elucidate information on the etiologies and mechanisms of human diseases, especially for those that are difficult to access in patients, including ovarian cancer.[19] However, the lack of a feasible spontaneous model of human ovarian cancer represents one of the principal barriers to the understanding of early ovarian tumor development and its detection. Ovarian cancer does not develop spontaneously in rodents, and the histopathologic characteristics of induced ovarian cancer in these animals do not resemble those of spontaneous ovarian cancer.[19,20] Laying hens (*Gallus domesticus*) have been shown to be the only widely available animal in which ovarian cancer develops spontaneously,[21] with similar histopathologic characteristics[22] and expression of several cellular and molecular makers common to human ovarian tumors.[23–26] Moreover, the incidence rate increases with age (10%–40% between 2.5 and 6 years of age).[21] The high ovulation rate in commercial strains of laying hens (a hen lays an egg almost every day with an ovulatory cycle of about 24–26 hours during its reproductive life) also mimics the incessant ovulation theory (a condition referring to frequent ovulation resulting in repeated trauma as well as wear and tear of the ovarian surface epithelium[27]), a much-accepted risk factor for ovarian cancer in humans (detailed descriptions of the reproductive physiology of laying hens have been published else where[21,22]). Recently, a transvaginal Doppler

sonographic method for hen ovarian tumors using a transducer similar to that used for humans has been reported.[28] As in humans, tissue expression of vascular endothelial growth factor (VEGF), a marker of ovarian tumor-associated neoangiogenesis, has also been shown to be increased in association with tumor progression in hens.[4,26] In addition, laying hens are easily accessible, especially because commercial poultry farms maintain large populations of hens, which they usually cull when hens get older. Therefore, the laying hen represents a potentially feasible surrogate for exploring information related to contrast-enhanced sonography for diagnosis of ovarian cancer at early stages, which is difficult to perform in humans.

The goal of this pilot study was to examine the feasibility of using laying hens to determine the kinetics of ultrasound contrast agents indicative of ovarian tumor-associated neoangiogenesis in early-stage ovarian cancer. We hypothesized that the ultrasound contrast agent Optison (GE Healthcare, St Louis, MO) would enhance the visualization of ovarian vascularity in the laying hen relative to ovarian cancer.

Materials and Methods

Animals

Approximately 150 White Leghorn laying hens (*G domesticus*, commercial strains, 3 years old) were maintained in individual cages with standard poultry husbandry practices, including the provision of feed and water ad libitum. The egg-laying rates (an indicator of ovarian function; a low egg-laying rate indicates decreased ovarian function) of the hens were recorded on a daily basis. The normal rate of egg laying by a commercial laying hen is more than 250 eggs per year, and less than 50% of the normal laying rate is considered a low egg-laying rate.[4,29] Hens (n = 46) with low, irregular egg-laying rates and those that stopped laying, with or without any abdominal distention (a sign of possible ovarian tumor-associated ascites), were selected randomly from a laying flock for ultrasound scanning. The incidence of ovarian cancer in laying hens of this age group was reported to be approximately 15% to 20% and is associated with low or complete cessation of egg laying.[22,30]

Preparation of Optison

Optison is a sterile nonpyrogenic suspension of 3.0- to 4.5-μm microspheres of human serum albumin with perflutren protein type A, which create an echogenic contrast effect in blood. Optison was prepared before injection according to the manufacturer's directions. Briefly, the vial containing the Optison suspension was inverted and gently rotated to resuspend the microspheres completely. The suspension was transferred from the vial by an injection syringe with a 19-gauge needle to a angiocatheter (small-vein infusion set, female luer, 12-in tubing, 27-gauge needle; Kawasumi Laboratories, Tampa, FL) containing 100 μL of 0.9% sodium chloride previously inserted into the left wing vein (brachial vein) of the hen and followed by the reloading of 1 mL of a 0.9% sodium chloride solution. The loading of the sodium chloride solution before and after injection of Optison helped maintain the vascular patency and airtight condition, in addition to flushing the Optison from the hen's circulation. The dose of Optison was determined after prior attempts with several doses using 5 laying hens with fully functional ovaries, and 5 μL/kg body weight was considered optimal for better resolution. With the dose higher than 5 μL/kg, the initial arrival of Optison caused an excessive broadening of color areas (blooming, due to an increase in the flow signal strength).[13,31,32] The blooming effect was detected when gray scale pixels changed to a color display in regions where no flow in fact existed. Although the exact borders of enhanced vessels often vanished in a few hens at the 5–μL/kg dose, blooming

was not intense enough to disturb vessel number counting. Blooming effects were also reported in previous studies.

Sonography

Precontrast Scanning—All procedures were performed according to Institutional Animal Care and Use Committee approval. Sonography was performed in a continuous pattern before and after the injection of Optison[4,28] with the mechanical set up reported previously. Briefly, all hens were scanned using an instrument equipped with a 5- to 7.5-MHz endovaginal transducer (MicroMaxx; SonoSite, Inc, Bothell, WA). Each hen was immobilized by being placed with the breast up and legs gently restrained by an assistant. Transmission gel was applied to the surface of the transducer; a probe cover was applied; and gel was reapplied to the covered probe to ensure uninterrupted conductance of the sound waves. The transducer was inserted approximately at a 30° angle to the body, 3 to 5 cm into the cloaca (transvaginal), and 2-dimensional transvaginal gray scale sonography as well as pulsed Doppler sonography were performed. Young egg-laying hens (because the ovaries of these hens contain more developing follicles compared to old hens) were used as standard controls for mechanical adjustment to reveal and characterize the fully functional normal ovaries of hens. The area of a tumor to be imaged was determined according to 3 conditions: (1) the whole tumor should be seen on the image, if possible; (2) the sectional plane should contain the solid part (wall, septa, and papillae) of the tumor; and (3) the most vascularized area was selected. For normal ovaries, ovaries without any detectable tumor, and atrophied ovaries, the region surrounding the ovary was scanned, and the transducer was swept through the entire area for complete scanning of the ovary. Gray scale morphologic evaluation of the ovarian mass was performed with attention to the number of large preovulatory follicles, the presence of abnormal-looking follicles, bilaterality, septations, papillary projections or solid areas, and echogenicity. After morphologic evaluation, the color Doppler mode was activated for identification of vascular color signals. If blood flow was detected, it was shown as either "peripheral" (color signals in the wall or periphery of a follicle or a suspected mass) or "central" (blood flow detected in septa, papillary projections, or solid areas). Once a vessel was identified on color Doppler imaging, the pulsed Doppler gate was activated to obtain a flow velocity waveform. The resistive index (RI: [systolic velocity – diastolic velocity]/systolic velocity) and the pulsatility index (PI: [systolic velocity – diastolic velocity]/mean) were automatically calculated from at least 2 consecutive samples (2 separate images from the same ovary), and the lower RI and PI values were used for analysis. All images were processed and digitally archived.

Postcontrast Scanning—Post-Optison injection scanning was performed in a similar and continuous manner with identical mechanical settings as described above. The same precontrast imaged area was imaged after Optison injection in postcontrast scanning. All images were archived digitally in a still format as well as real-time clips (6 minutes for each hen) on single-sided recordable digital video disks (DVD+R format; Maxell Corporation of America, Fair Lawn, NJ) readable on a personal computer later.

Evaluation of the Contrast Agent Effect

The effect of Optison was evaluated visually during the examination and afterward from reviewing the archived video clips. The time of contrast agent arrival (interval in seconds from administration of the contrast agent to its visual observation [in seconds]) in the normal and tumorous ovarian vessels was recorded in real time. After review of the complete clip, the region of interest was selected by drawing around the area of solid tissue containing the largest number of vessels with minimal artifacts similar to those reported earlier.[14,17] For normal or apparently normal (without a detectable tumor mass on gray scale imaging) ovaries, stromal but not follicular vessels were counted. A color area separated from others

with a distinct wall typical of a blood vessel was assessed before and after injection of the contrast agent. Therefore, the postcontrast appearance of blood vessels in this study could have been either new vessels or branches of vessels already recognized before administration of the contrast agent. Analysis of pixel intensities of blood vessels was performed with computer-assisted software (MicroSuite version 5; Olympus Corporation, Tokyo, Japan). Using the software, the intensity of the region of interest (sum of the pixel values within the region of interest) was measured before contrast agent administration and at intervals of 5 seconds after arrival of the contrast agent up to 6 minutes. Then the peak intensity, time of peak intensity (seconds), intensity at wash-out, and time of wash-out (seconds) were determined. The total number of blood vessels from each region of interest was counted when the intensity was at its peak. In addition, the RI and PI were calculated before and after the contrast agent injection using a previously reported formula.[28]

The data were then transferred to a computerized spreadsheet program (Excel 2003; Microsoft Corporation, Redmond, WA) and a time-intensity curve was derived for each hen. The time-intensity curves were analyzed to calculate areas under the curves (AUCs). The AUCs diagnostic of ovarian cancer in hens were derived from the arrival of the contrast agent and the end of the wash-out period minus the area under the baseline in the time-intensity curve.

Ovarian Morphologic Evaluation

After sonography, all hens were euthanized and examined for the presence of a solid tumor mass in the ovary and any other organs, ascitic fluid, large preovulatory follicles, and atrophy of the ovary, as reported previously.[22] The gross ovarian status was recorded and compared to the sonographic evaluations and photographed. At gross examination, an ovary of a laying hen is considered normally functional if it contains viable large preovulatory follicles (more detailed information on hen ovarian physiology has been published elsewhere[21,22]), whereas atrophy of the ovary without any large follicles or visible lesions is characteristic of hens out of egg laying. In contrast to a normal ovary, an abnormal ovary was characterized by the presence of cysts or bloody, discolored, involuted, or atretic large preovulatory, small, and pear-shaped follicles. Tumor staging was performed according to the gross metastatic status and histologic observations, as reported previously.[22] Briefly, early ovarian cancer (stage 1 or 2) was characterized by detectable formation of a solid tumor in the ovary or extensive tumors but still restricted to the ovary. Late stages of ovarian cancer were characterized by tumor metastasis to distant organs with moderate to extensive ascites.

Ovarian Histopathologic Evaluation and Immunohistochemical Detection of Ovarian Microvessel Density

Representative portions of a solid ovarian mass or the whole ovary (in cases of atrophied or apparently normal-appearing ovaries) were divided into several blocks, processed for paraffin sections, and stained with hematoxylin-eosin. Microscopic tumor lesions in any part of the ovary were detected by routine histologic examination with hematoxylin-eosin staining, and tumor types were determined by light microscopy, as reported previously.[22]

After histopathologic examination, paraffin sections (5 μm thick) of normal and tumorous ovaries of all stages and types were processed for routine immunohistochemistry to assess the tumor-associated microvessel density using a monoclonal anti-α-smooth muscle actin antibody (primary antibody; Invitrogen, Carlsbad, CA) according to the manufacturer's protocols. The densities of immunopositive microvessels were counted from the tumor vicinity or stroma of normal hens (excluding the follicular areas), as reported earlier[33,34] using a light microscope attached to digital imaging stereologic software (MicroSuite

version 5; Olympus Corporation) with a little modification. Briefly, immunostained slides were examined at low-power magnification (×10 objective and ×10 ocular) to identify the areas of maximum neovascularization of the tumor. Vessels with thick, regular, and complete muscular walls as well as vessels with large lumina were excluded from the count, as reported previously.[34] Brown-stained leaky smaller vessels with discontinuous or incomplete vessel walls, clearly separated from adjacent microvessels, tumor cells, and other connective tissue elements, were considered a single countable vessel. In each section, the 5 most vascular areas were chosen. The number of microvessels in a 20,000-μm^2 area was counted at a ×40 objective and ×10 ocular magnification. The averages of these counts were expressed as the number of immunopositive microvessels in a 20,000-μm^2 area of a normal or tumorous ovary. Tumor histologic and immunohistochemical observations were compared to the sonographic predictions.

Statistical Analysis

Descriptive statistics for contrast parameters were determined, and statistical analysis was performed in SPSS version 15 statistical software (SPSS Inc, Chicago, IL). The differences between the power Doppler intensity changes before and after contrast agent injection were analyzed by the paired *t* test and the exact sign test. The differences in the contrast parameters and the density of immunopositive microvessels between normal and tumorous ovaries were analyzed by the 2-sample *t* test and the exact Mann-Whitney test. The χ^2 test was used to investigate the association between the contrast parameters, including the wash-out time and AUC, with the presence or absence of a tumor lesion. $P < .05$ was considered significant. All reported *P* values are 2 sided.

Results

Sonography

Optison injected at a dose of 5 μL/kg body weight was well tolerated, and none of the hens showed any adverse conditions.

Normal and Tumorous Ovaries in Hens

Normal ovaries in healthy hens (n = 24) were found to have multiple preovulatory follicles with many small growing stromal follicles on gray scale sonography. Blood vessels were detected in the ovarian stroma on Doppler imaging (Figure 1A). In addition, confluent blood flow was detected on the surfaces of large preovulatory follicles. Compared to precontrast scans, Optison injection enhanced visualization of ovarian blood vessels in the same area of the ovary (Figure 1B). Solid ovarian masses with or without projected septa and papillary structures, accompanying ascites, or both were observed in the ovaries of 15 hens on gray scale and Doppler sonography, and these hens were "predicted to have ovarian tumors" (Figure 1C). No large preovulatory follicles were observed in these hens. Of these 15 hens, 11 had solid masses in the ovary together with profuse ascites and were categorized as having late-stage ovarian cancer. In the remaining 4 hens, solid masses were found to be limited to a part of the ovary without any detectable ascites, and they were categorized provisionally as early-stage ovarian cancer (final diagnosis performed on gross examination). Optison injection remarkably enhanced visualization of ovarian tumor-associated vascular networks in all hens predicted to have ovarian cancer (Figure 1D).

The ovaries in a few hens (n = 7) appeared regressed, with only 1 or no large preovulatory follicle. Although no detectable solid ovarian mass was observed on gray scale sonography in these hens, their RI and PI values were lower than those of the hens with normal ovaries. These hens were termed "hens with abnormal ovarian morphologic characteristics" because their diagnosis was not conclusive by sonography (Figure 2) and subsequent histopathologic

examinations (detailed below) showed the presence of microscopic malignant tumor lesions in a portion of the ovaries of these hens. Thus, these hens were finally categorized as "hens with microscopic ovarian cancer." The precontrast and postcontrast RI and PI values were significantly lower in hens suspected to have ovarian cancer compared to their normal counterparts ($P < .01$, exact Mann-Whitney test; Table 1).

Contrast Parameters

Number of Blood Vessels—Overall, compared to precontrast findings, the numbers of detectable blood vessels in the normal as well as the tumorous ovaries were significantly increased after Optison injection ($P < .05$; Table 1). Compared to normal hens, significantly more blood vessels were observed in hens predicted to have ovarian tumors ($P < .05$), and their frequencies increased as the tumors progressed from microscopic to later stages (Table 1).

Doppler Intensity and Contrast Kinetics

Compared to precontrast findings, Optison injection significantly enhanced the power Doppler intensity signal to greater than 2-fold in all hens irrespective of their pathologic status ($P < .05$; Figure 3). Compared to normal hens, the intensity of postcontrast Doppler signals was highest in hens predicted to have ovarian tumors ($P < .05$; Figure 3).

Although the time of arrival and time to reach peak intensity of the contrast agent tended to be faster in hens predicted to have ovarian tumors than normal hens, the difference was not statistically significant (Table 2). The wash-out of the contrast agent had 2 phases: a fast initial decrease and a second slower decrease approximately to the baseline. The wash-out of Optison was shorter in normal hens and was significantly longer in hens predicted to have ovarian tumors ($P < .05$; Table 2). Compared to normal hens, a significantly greater AUC was observed in hens predicted to have ovarian tumors ($P < .05$; Table 2). Differences were not observed among hens with different tumor types (serous, endometrioid, mucinous, and seromucinous mixed) with respect to their contrast parameters

Histopathologic Findings and Microvessel Density

Gross examination of hens at necropsy confirmed the sonographic predictions. Ovarian tumors, their stages, and types were confirmed at necropsy and by routine histologic examination with hematoxylin-eosin staining, respectively (Figure 4). As observed on sonography, late-stage ovarian cancer (n = 11 hens: 4 serous, 5 endometrioid, 1 mucinous, and 1 seromucinous mixed) was associated with moderate to profuse ascites and metastasis to distant organs. Early-stage ovarian cancer (n = 4 hens) was limited to the ovary (1 serous, 1 endometrioid, and 2 seromucinous mixed) with little or no ascites. The 7 hens initially classified as hens with abnormal ovarian morphologic characteristics without any grossly detectable solid ovarian masses during gray scale sonography had microscopic malignant ovarian lesions on hematoxylin-eosin staining in 1 or more areas of the ovary and thus were classified as hens with microscopic ovarian cancer.

Immunopositive microvessels were detected in both normal ovaries and ovarian tumors (Figure 5). In normal hens, most of the immunopositive ovarian vessels had thick, complete, and continuous vessel walls with intense staining. In contrast, most of the vessels in ovarian tumors were leaky, discontinuous, or incomplete with thin vessel walls (Figure 5). In normal hens, most of the immuno-positive microvessels were located in the follicular theca, with few positive blood vessels in the ovarian stroma. The densities of immunopositive ovarian microvessels were significantly higher ($P < .01$, exact Mann-Whitney test) in hens predicted to have ovarian tumor-associated neoangiogenesis on contrast-enhanced sonography (mean ± SD, 8.0 ± 0.53, 13.0 ± 0.84, and 19.0 ± 1.3 microvessels per 20,000-μm^2 area of ovarian

tumor tissues in microscopic, early-stage, and late-stage ovarian cancer, respectively) than normal hens (4.0 ± 0.55 microvessels per 20,000-μm^2 area of ovarian tissues). In addition to immunopositive microvessels, smooth muscle fibers surrounding the tumor glands but not the tumor epithelium also stained positively. However, differences were not observed among different tumor types with regard to their immunopositive microvessel densities. Thus, increased numbers of ovarian microvessels in tumorous ovaries compared to normal ovaries confirmed the in vivo prediction of ovarian tumor-associated neoangiogenesis by contrast-enhanced sonography.

In Vivo Detection of Ovarian Tumor-Associated Neoangiogenesis

The pathologic status of hens, including tumor staging (by histopathologic examination) and tissue expression of ovarian microvessels (by immunohistochemistry) were compared to contrast parameters. Data on 3 contrast parameters, including the peak postcontrast Doppler intensity, wash-out time of the contrast agent, and AUC, were used retrospectively to determine the efficacy of the contrast parameters in detecting in vivo ovarian tumor-associated neoangiogenesis. Two cutoff values for each of these 3 contrast parameters, namely, the mean ± 2 SDs and mean ± 3 SDs of the peak intensity value and wash-out time or AUC of normal (control) hens, were used to examine the detectability of ovarian tumor-associated neoangiogenesis at an early stage of ovarian cancer. All 3 parameters with both the cutoff values were detected in all hens with ovarian cancer in an early stage (tumor detected at gross examination and limited to the ovary) or late stage. The cutoff value for the peak postcontrast Doppler intensity ± 2 SDs identified 86% (6 of 7) of the hens with microscopic lesions (without any detectable tumor on gray scale sonography or gross examination at euthanasia), whereas those with 3 SDs identified only 43% (3 of 7) of these hens (Figure 3). On the other hand, the cutoff value for the AUC with 3 SDs identified 86% of the hens with microscopic ovarian cancer (Table 2). However, the wash-out time of the contrast agent identified all hens with microscopic ovarian cancer using both cutoff values (Table 2 and Figure 6). Thus, the AUC and wash-out time of the contrast agent were found to be more efficient for detection of microscopic ovarian cancer than the other contrast parameters.

Discussion

To our knowledge, a study on the improvement of in vivo detection of ovarian tumor-associated vascular architecture with the ultrasound contrast agent Optison in laying hens, a spontaneous animal model of human ovarian cancer, has not been reported previously. Our goals were to test the efficacy of the contrast agent in enhancing the visualization of ovarian tumor-associated blood vessels in laying hens and to determine the contrast kinetics associated with early-stage ovarian cancer in laying hens. The results of this study suggest that the contrast agent enhanced the detection of the hen ovarian vascular network. Our results also suggest that laying hens provide a new and valid platform for studying kinetic parameters relative to early-stage ovarian cancer using a contrast agent. The translational importance of this study is that the laying hen may be a suitable preclinical model of spontaneous human ovarian cancer for the study of contrast-enhanced sonography to establish an early detection test for ovarian cancer. This animal model of spontaneous ovarian cancer may also be useful for testing the efficacy of different contrast agents in vivo in a preclinical setting.

In this study, compared to precontrast scanning, the significant enhancement in the detection of ovarian microvessels by power Doppler sonography using a contrast agent without any adverse physiologic effects suggests the utility of this contrast agent in hens, as reported in humans. The time of wash-out of the contrast agent and the AUC were significantly different between hens with ovarian tumors and hens with normal ovaries. Similar patterns

were also reported in patients with ovarian cancer.[13,14] Ovarian RI and PI values decreased in hens with normal and tumorous ovaries after the contrast agent injection irrespective of their disease status. Although the precise reason(s) is not known, it is possible that the increase in the amount of recognizable vessels and increased blood flow may be the factors responsible for such a decrease in RI and PI values after contrast agent injection. Lower RI and PI values in hen ovarian tumors than in hen normal ovaries also support previous findings that lower RI and PI values are associated with ovarian cancer[4,28]; thus, these indices may be used together with the contrast parameters to distinguish malignant ovarian vasculature from that of the normal ovary. Decreased RI and PI values in association with increased numbers of blood vessels (immunohistochemical observation) confirmed the enhanced detection of ovarian tumor-associated vascular networks by contrast parameters using Optison. Thus, the tolerance as well as the enhanced detection of ovarian blood vessels by the contrast agent in hens, as in humans, suggests the suitability of laying hens as a preclinical animal model to study the contrast kinetics diagnostic of early-stage ovarian cancer.

Ovarian tumor-associated neoangiogenesis is the hallmark of tumor development and progression. Contrast parameters, including the time of wash-out of the contrast agent and the AUC, as observed in this study, may be useful in distinguishing normal ovarian physiologic angiogenesis from the ovarian tumor-associated neoangiogenesis at early stages of ovarian cancer. An increase in leaky and immature ovarian microvessels, as observed in this study, is one of the characteristics of ovarian tumor-associated neoangiogenesis.[1,35] These increased microvessel densities were associated with contrast parameters predictive of ovarian tumors. Recently, we have reported that ovarian tumor progression in hens is associated with an increased frequency of VEGF-expressing ovarian blood vessels.[4] Thus, an increase in ovarian microvessel frequency (as observed in this study) together with the increased expression of VEGF by these microvessels[4] may suggest that VEGF also plays a critical role in ovarian tumor progression in laying hens, as in humans. Therefore, VEGF represents an additional marker of ovarian cancer. Elevated concentrations of circulatory VEGF have been reported to be associated with ovarian cancer in humans. Although not determined in this study, a serum VEGF concentration may identify which hens are at risk of ovarian cancer development and may be followed prospectively with sonographic monitoring for detecting ovarian cancer-related morphologic changes in the ovary. Because VEGF is not specific for ovarian tumor-associated neoangiogenesis only, it is possible that circulatory VEGF screening (a marker of tumor-associated neoangiogenesis) in association with other techniques such as contrast-enhanced sonography may constitute an effective early detection test for ovarian cancer. The laying hen may be useful in establishing this early detection test. Recently, we generated antichicken VEGF antibodies to detect serum concentrations of VEGF by an immunoassay in chickens. Thus, the findings of this study may facilitate future studies with elevated circulatory VEGF concentrations for monitoring hens prospectively to detect the development of ovarian cancer at an early stage and to establish an early detection test in this preclinical model.

The small number of hens (total, 46: 24 normal and 7 microscopic, 4 early-stage, and 11 late-stage ovarian cancer) used was a limitation of this study. We used both the paired *t* test and its nonparametric equivalent, the exact sign test, for before and after comparison of Optison's effects. Similarly, we used both the 2-sample *t* test and its nonparametric equivalent, the exact Mann-Whitney test, for comparing normal versus tumorous ovaries. The reported significant results were typically found in both the *t* test (paired or 2 sample, as appropriate) and the nonparametric test (sign test or Mann-Whitney test). The *P* for the exact sign test and exact Mann-Whitney test are computed by numerical methods without any large sample approximations and are valid in small samples. Thus, the remarkable increase in the intensity of the ovarian vascular architecture as well as the number of blood vessels

after contrast agent injection may form the foundation for a larger study to establish an effective early detection test for ovarian cancer. Furthermore, laying hens may also be useful in developing ovarian tumor-associated neoangiogenesis–targeted molecular imaging and monitoring the effects of antiangiogenic drugs related to the recession or relapse of ovarian tumors.

A few reports have stated that Doppler imaging using contrast agents to assess tumor enhancement has low contrast and resolution, substantial background noise, and considerable operator dependence and suggested that these limitations can be addressed by new sonographic imaging methods, such as pulse inversion harmonic imaging.[11,14,35] Although we have not used the pulse inversion harmonic method, we adjusted the dose of Optison for optimal contrast and resolution with minimum background noise in our initial studies using this model.

In conclusion, the results of this pilot study show that the laying hen, a preclinical animal model of spontaneous human ovarian cancer, may be useful for understanding and determining ovarian tumor-associated vascular kinetics during early- and late-stage ovarian cancer using contrast-enhanced sonography. Information on contrast-enhanced sonography for detection of early-stage ovarian cancer in laying hens will also provide a foundation for clinical studies.

Abbreviations

AUC	area under the curve
PI	pulsatility index
RI	resistive index
VEGF	vascular endothelial growth factor

Acknowledgments

We thank Chet and Pam Utterback and Doug Hilgendorf, staff of the University of Illinois at Urbana-Champaign Poultry Research Farm, for maintenance of the hens. We also thank Sergio Abreu Machado, graduate student, Department of Animal Sciences, University of Illinois at Urbana-Champaign, for help in injecting hens with Optison.

This study was supported by the Prevent Cancer Foundation (Dr Barua), Rush University Research Committee grants in aid (Dr Barua), the Brian Piccolo Cancer Research Fund (grants for purchasing the ultrasound machine, Dr Barua), National Cancer Institute Pacific Ovarian Cancer Research Consortium Career Development Program grant P50 CA83636 (to Dr Barua; principal investigator, Nicole Urban, ScD) and the Elmer Sylvia and Sramek Foundation (Dr Barua).

References

1. Folkman J. What is the evidence that tumors are angiogenesis dependent? J Natl Cancer Inst. 1990; 82:4–6. [PubMed: 1688381]
2. Shubik P. Vascularization of tumors: a review. J Cancer Res Clin Oncol. 1982; 103:211–226. [PubMed: 6181069]
3. Ramakrishnan S, Subramanian IV, Yokoyama Y, Geller M. Angiogenesis in normal and neoplastic ovaries. Angiogenesis. 2005; 8:169–182. [PubMed: 16211363]
4. Barua A, Bitterman P, Bahr JM, et al. Detection of tumor-associated neoangiogenesis by Doppler ultrasonography during early-stage ovarian cancer in laying hens: a preclinical model of human spontaneous ovarian cancer. J Ultrasound Med. 2010; 29:173–182. [PubMed: 20103787]
5. Jemal A, Siegel R, Ward E, Hao Y, Xu J, Thun MJ. Cancer statistics, 2009. CA Cancer J Clin. 2009; 59:225–249. [PubMed: 19474385]

6. Hata K, Fujiwaki R, Maede Y, Nakayama K, Fukumoto M, Miyazaki K. Expression of thymidine phosphorylase in epithelial ovarian cancer: correlation with angiogenesis, apoptosis, and ultrasound-derived peak systolic velocity. Gynecol Oncol. 2000; 77:26–34. [PubMed: 10739687]
7. Hata K, Fujiwaki R, Nakayama K, Maede Y, Fukumoto M, Miyazaki K. Expression of thymidine phosphorylase and vascular endothelial growth factor in epithelial ovarian cancer: correlation with angiogenesis and progression of the tumor. Anticancer Res. 2000; 20:3941–3949. [PubMed: 11268481]
8. Bamberger ES, Perrett CW. Angiogenesis in epithelian ovarian cancer. Mol Pathol. 2002; 55:348–359. [PubMed: 12456770]
9. Bosse K, Rhiem K, Wappenschmidt B, et al. Screening for ovarian cancer by transvaginal ultrasound and serum CA125 measurement in women with a familial predisposition: a prospective cohort study. Gynecol Oncol. 2006; 103:1077–1082. [PubMed: 16904167]
10. Moore RG, Bast RC Jr. How do you distinguish a malignant pelvic mass from a benign pelvic mass ? Imaging, biomarkers, or none of the above. J Clin Oncol. 2007; 25:4159–4161. [PubMed: 17698803]
11. Fleischer AC, Lyshchik A, Jones HW, et al. Diagnostic parameters to differentiate benign from malignant ovarian masses with contrast-enhanced transvaginal sonography. J Ultrasound Med. 2009; 28:1273–1280. [PubMed: 19778872]
12. Fishman DA, Cohen L, Blank SV, et al. The role of ultrasound evaluation in the detection of early-stage epithelial ovarian cancer. Am J Obstet Gynecol. 2005; 192:1214–1222. [PubMed: 15846205]
13. Orden MR, Gudmundsson S, Kirkinen P. Contrast-enhanced sonography in the examination of benign and malignant adnexal masses. J Ultrasound Med. 2000; 19:783–788. [PubMed: 11065267]
14. Marret H, Sauget S, Giraudeau B, et al. Contrast-enhanced sonography helps in discrimination of benign from malignant adnexal masses. J Ultrasound Med. 2004; 23:1629–1639. [PubMed: 15557306]
15. Leen E. Ultrasound contrast harmonic imaging of abdominal organs. Semin Ultrasound CT MR. 2001; 22:11–24. [PubMed: 11300584]
16. leischer AC, Lyshchik A, Jones HW Jr, et al. Contrast-enhanced transvaginal sonography of benign versus malignant ovarian masses: preliminary findings. J Ultrasound Med. 2008; 27:1011–1018. [PubMed: 18577664]
17. Orden MR, Jurvelin JS, Kirkinen PP. Kinetics of a US contrast agent in benign and malignant adnexal tumors. Radiology. 2003; 226:405–410. [PubMed: 12563133]
18. Suren A, Osmers R, Kulenkampff D, Kuhn W. Visualization of blood flow in small ovarian tumor vessels by transvaginal color Doppler sonography after echo enhancement with injection of Levovist. Gynecol Obstet Invest. 1994; 38:210–212. [PubMed: 8001878]
19. Vanderhyden BC, Shaw TJ, Ethier JF. Animal models of ovarian cancer. Reprod Biol Endocrinol. 2003; 1:67. [PubMed: 14613552]
20. Stakleff KD, Von Gruenigen VE. Rodent models for ovarian cancer research. Int J Gynecol Cancer. 2003; 13:405–412. [PubMed: 12911715]
21. Fredrickson TN. Ovarian tumors of the hen. Environ Health Perspect. 1987; 73:35–51. [PubMed: 3665870]
22. Barua A, Bitterman P, Abramowicz JS, et al. Histopathology of ovarian tumors in laying hens: a preclinical model of human ovarian cancer. Int J Gynecol Cancer. 2009; 19:531–539. [PubMed: 19509547]
23. Rodriguez-Burford C, Barnes MN, Berry W, Partridge EE, Grizzle WE. Immunohistochemical expression of molecular markers in an avian model: a potential model for preclinical evaluation of agents for ovarian cancer chemoprevention. Gynecol Oncol. 2001; 81:373–379. [PubMed: 11371125]
24. Jackson E, Anderson K, Ashwell C, Petitte J, Mozdziak PE. CA125 xpression in spontaneous ovarian adenocarcinomas from laying hens. Gynecol Oncol. 2007; 104:192–198. [PubMed: 16942793]
25. Hales DB, Zhuge Y, Lagman JA, et al. Cyclooxygenases expression and distribution in the normal ovary and their role in ovarian cancer in the domestic hen (Gallus domesticus). Endocrine. 2008; 33:235–244. [PubMed: 18498063]

26. Urick ME, Giles JR, Johnson PA. VEGF expression and the effect of NSAIDs on ascites cell proliferation in the hen model of ovarian cancer. Gynecol Oncol. 2008; 110:418–424. [PubMed: 18606441]
27. Fathalla MF. Incessant ovulation: a factor in ovarian neoplasia? Lancet. 1971; 2:163. [PubMed: 4104488]
28. Barua A, Abramowicz JS, Bahr JM, et al. Detection of ovarian tumors in chicken by sonography: a step toward early diagnosis in humans? J Ultrasound Med. 2007; 26:909–919. [PubMed: 17592054]
29. Bahr JM, Palmer SS. The influence of aging on ovarian function. Crit Rev Poult Biol. 1989; 2:8–14.
30. Damjanov I. Ovarian tumours in laboratory and domestic animals. Curr Top Pathol. 1989; 78:1–10. [PubMed: 2651020]
31. Forsberg F, Liu JB, Burns PN, Merton DA, Goldberg BB. Artifacts in ultrasonic contrast agent studies. J Ultrasound Med. 1994; 13:357–365. [PubMed: 8015042]
32. Orden MR, Gudmundsson S, Kirkinen P. Intravascular ultrasound contrast agent: an aid in imaging intervillous blood flow? Placenta. 1999; 20:235–240. [PubMed: 10195747]
33. Weidner N, Folkman J, Pozza F, et al. Tumor angiogenesis: a new significant and independent prognostic indicator in early-stage breast carcinoma. J Natl Cancer Inst. 1992; 84:1875–1887. [PubMed: 1281237]
34. Bosari S, Lee AK, DeLellis RA, Wiley BD, Heatley GJ, Silverman ML. Microvessel quantitation and prognosis in invasive breast carcinoma. Hum Pathol. 1992; 23:755–761. [PubMed: 1377162]
35. Schiffenbauer YS, Abramovitch R, Meir G, et al. Loss of ovarian function promotes angiogenesis in human ovarian carcinoma. Proc Natl Acad Sci USA. 1997; 94:13203–13208. [PubMed: 9371824]

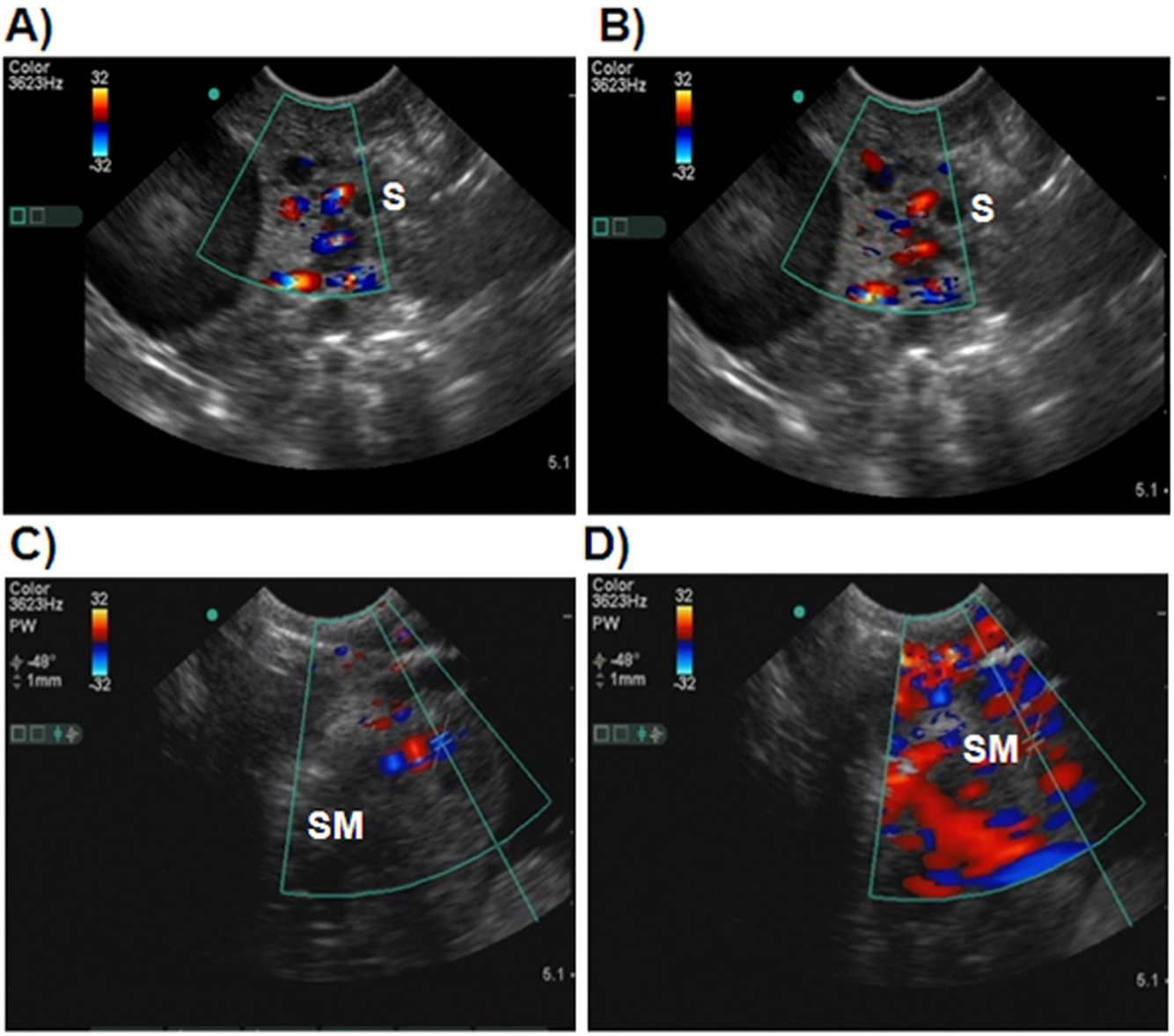

Figure 1.

Precontrast and postcontrast Doppler sonograms of hen ovaries with and without tumors. Scanning of hens was performed in a continuous manner before and after injection of Optison. Images including still and movie clips were digitally archived. Contrast kinetics, namely, the time of arrival, time to reach peak intensity, and time of wash-out, as well as precontrast and postcontrast Doppler indices (resistive and pulsatility index values) were recorded. **A**, Precontrast sonogram of a normal-appearing ovary showing a preovulatory follicle and few small follicles without any solid mass. **B**, Corresponding postcontrast sonogram from the same hen. Compared to the precontrast image, more vessels are shown in the postcontrast sonogram. **C**, Precontrast sonogram from a hen predicted to have an ovarian tumor. A solid tumorlike mass is shown in the ovary, and a central blood flow pattern with a few vessels is shown in and around the mass. **D**, Postcontrast sonogram of the ovary shown in **C**. The contrast agent remarkably enhances the intensity of blood vessels as well as visualization of more blood vessels. Compared to the precontrast image, many blood vessels

are shown in the postcontrast scan. Sonographic predictions were confirmed at gross (euthanasia) and histopathologic examination. S indicates stroma of the ovary; and SM, solid tissue mass in the ovary.

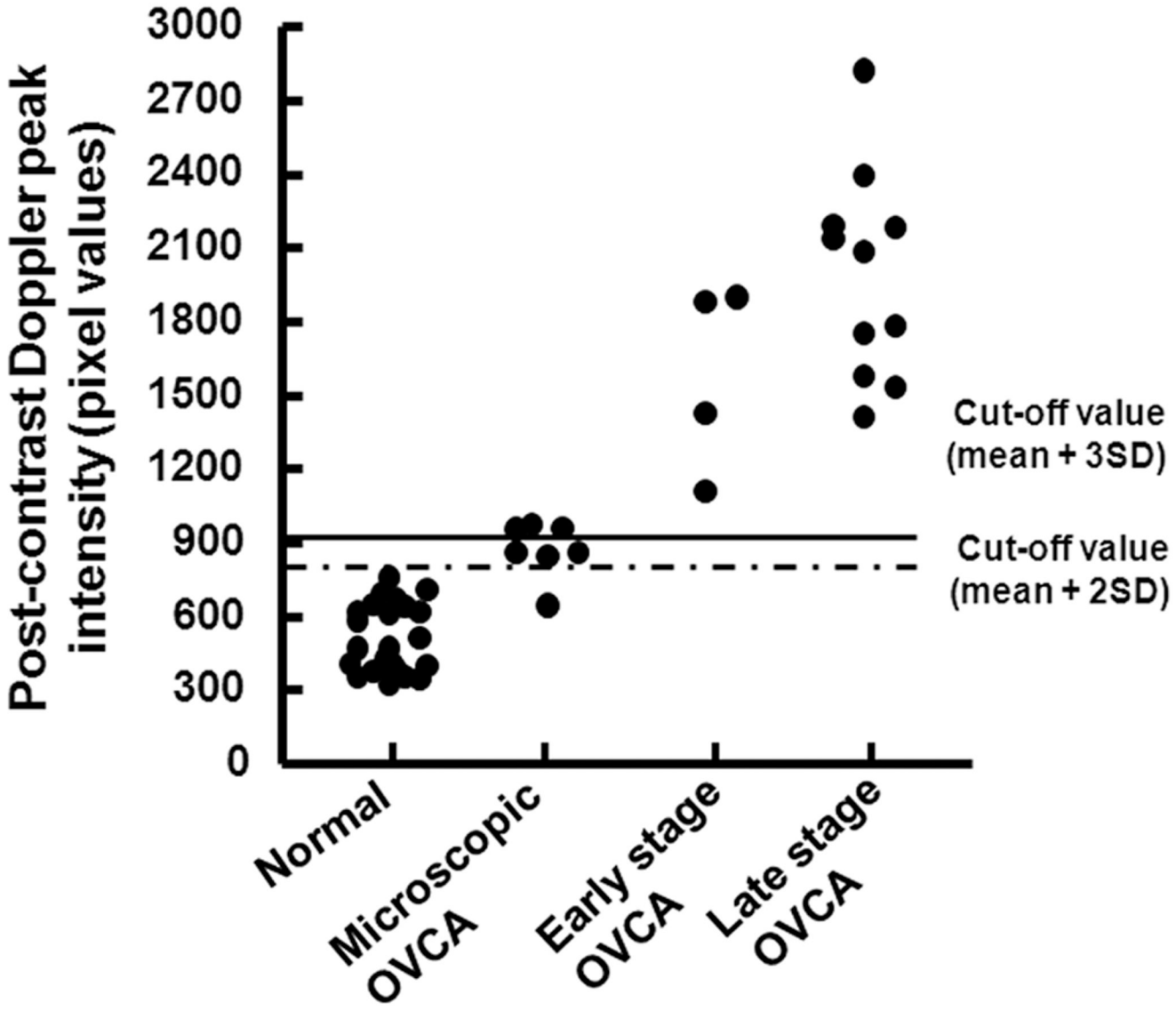

Figure 2.

The contrast agent (Optison) enhanced the ability of Doppler sonography to depict microscopic ovarian tumor-associated vasculature in laying hens. **A**, Precontrast sonogram of an ovary without a detectable solid ovarian mass or abnormality. Only a few blood vessels are shown in this ovary, with no preovulatory follicle. **B**, Corresponding sonogram of the same ovary showing the arrival of Optison. Compared to the precontrast image, the number of detectable blood vessels is increased, and the vessels appear more dilated in the postcontrast sonogram. **C**, Postcontrast sonogram of the same ovary showing the peak level of enhancement. Compared to the precontrast image and postcontrast image at the arrival of Optison, more vessels are shown at peak enhancement. Although no solid ovarian mass is shown, the central vascular arrangement pattern indicates a potential ovarian abnormality. **D**, Gross appearance of the same ovary at euthanasia. As predicted, neither a large preovulatory follicle nor a detectable solid mass is shown. However, subsequent histopathologic examination showed the presence of an endometrioid lesion (termed a microscopic ovarian tumor), confirming the contrast-enhanced sonographic prediction.

Scanning of hens and their subsequent processing were similar to those mentioned in Figure 1. Dotted circle indicates the ovary; and S, stroma.

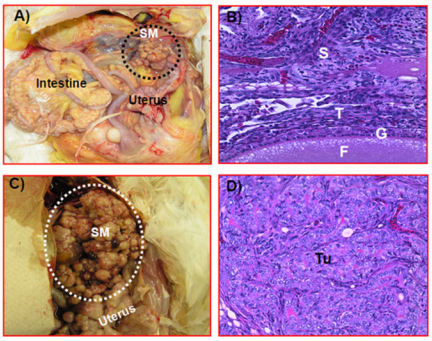

Figure 3.

Detection of ovarian tumor-associated neoangiogenesis by the postcontrast Doppler intensity of blood vessels. A flock of 150 hens were monitored for their ovarian function, and their egg-laying rates were recorded on a daily basis. Hens with low-egg laying rates (n = 46) were selected for sonography. On the basis of gray scale sonography and gross and histopathologic examinations, hens were grouped as having normal ovaries (n = 24 hens), microscopic ovarian cancer (OVCA; n = 7), early-stage ovarian cancer (n = 4), and late-stage ovarian cancer (n = 11). Postcontrast Doppler intensities of ovaries and ovarian tumors were measured by power Doppler sonography after Optison injection. Cutoff lines (mean peak Doppler intensity values of normal hens with 2 or 3 SDs) indicate the detectability of ovarian cancer by postcontrast peak Doppler intensities.

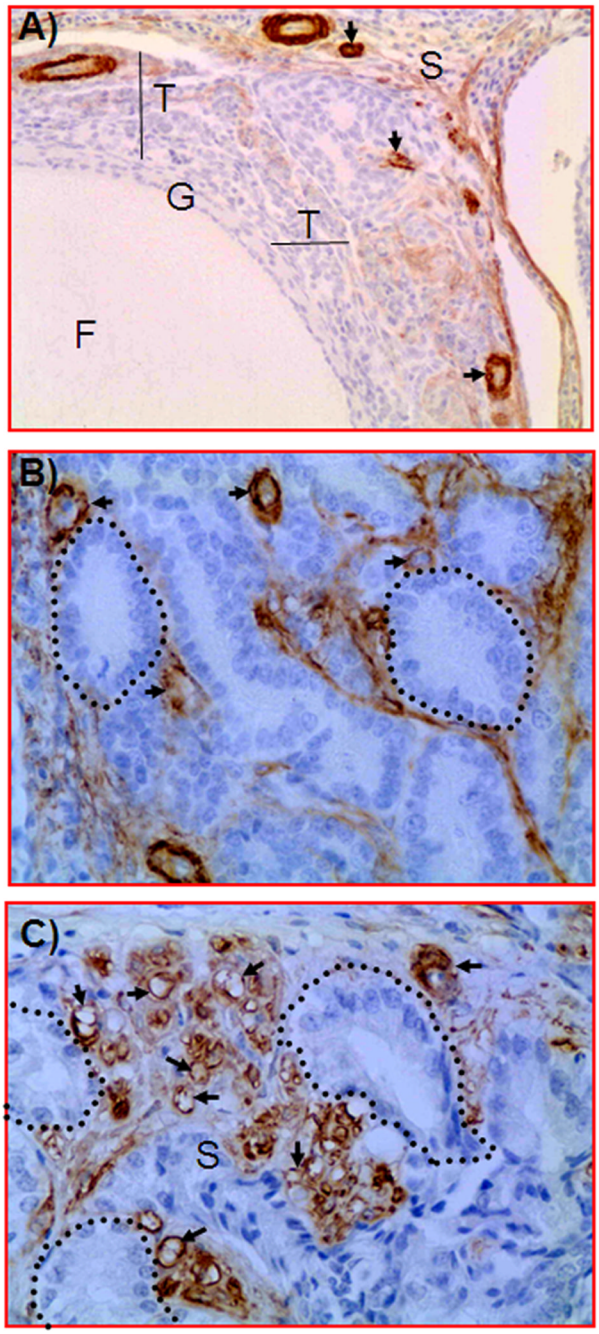

Figure 4.

Gross and histologic sections of ovarian tumors in hens scanned with contrast-enhanced sonography. After contrast-enhanced Doppler sonography, hens were euthanized and examined grossly for the presence of a tumor-related solid ovarian mass, which was confirmed by routine histologic examination with hematoxylin-eosin. **A**, Ovary of a hen with early-stage cancer. Few small solid tumor masses with no preovulatory follicles are present. The tumor is limited to a part of the ovary. **B**, Section taken from a normal and uninvolved portion of an ovary in which a tumor was detected in the other part of the ovary (early-stage ovarian cancer). Stromal follicles are embedded in the normal-appearing stroma. No invasion of tumor cells is shown in this portion of the ovary. **C**, Ovarian tumor

in a hen with late-stage ovarian cancer. The solid mass appears like a cauliflower. The tumor metastasized to distant organs and was associated with extensive ascites. **D**, Section of a serous ovarian tumor from a hen with late-stage ovarian cancer. The tumor has a compact sheath of tumor cells with pleomorphic nuclei, and tumor glands are surrounded by fibromuscular layers (hematoxylin-eosin; all sections: original magnification ×20). F indicates follicle; G, granulosa layer of the follicle; S, ovarian stroma; SM, solid tumor mass; T, theca layer of the follicle; and Tu, tumor.

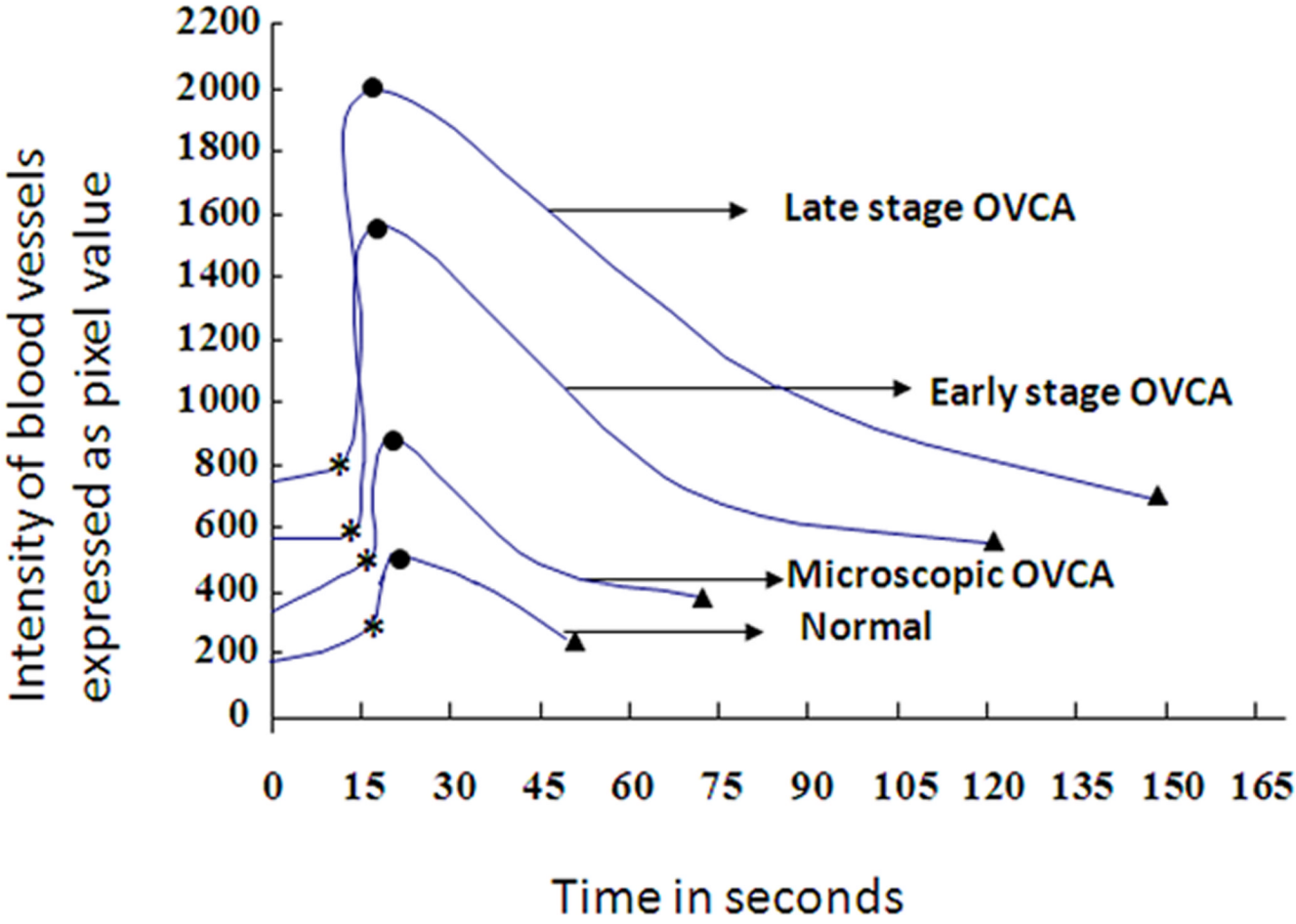

Figure 5.

Immunohistochemical detection of ovarian microvessels in laying hens with and without ovarian cancer. Paraffin sections were immunostained with monoclonal anti-smooth muscle actin. **A**, Section of a hen's normal ovary. Immunopositive microvessels are shown in the follicular theca and few in the adjacent stroma. Most of the immunopositive vessels have a thick wall. **B**, Section of a hen's ovary with early-stage ovarian cancer (ovary shown in Figure 4A). Compared to the normal ovary, more immature immunopositive microvessels with leaky, thinner, incomplete, or discontinuous vessel walls are present between tumor glands. The fibrous connective tissues of the tumor glands are also stained positive. **C**, Section of an ovarian tumor from a hen with late-stage ovarian cancer (ovary shown in Figure 4C). Compared to the normal ovary and early-stage ovarian cancer, many leaky and immature microvessels with discontinuous or attenuated staining are seen in the vicinity of the tumor. Arrows indicate examples of immunopositive microvessels; dotted circles, examples of tumor glands; F, follicle; G, granulosa layer; S, stroma; and T, theca layer.

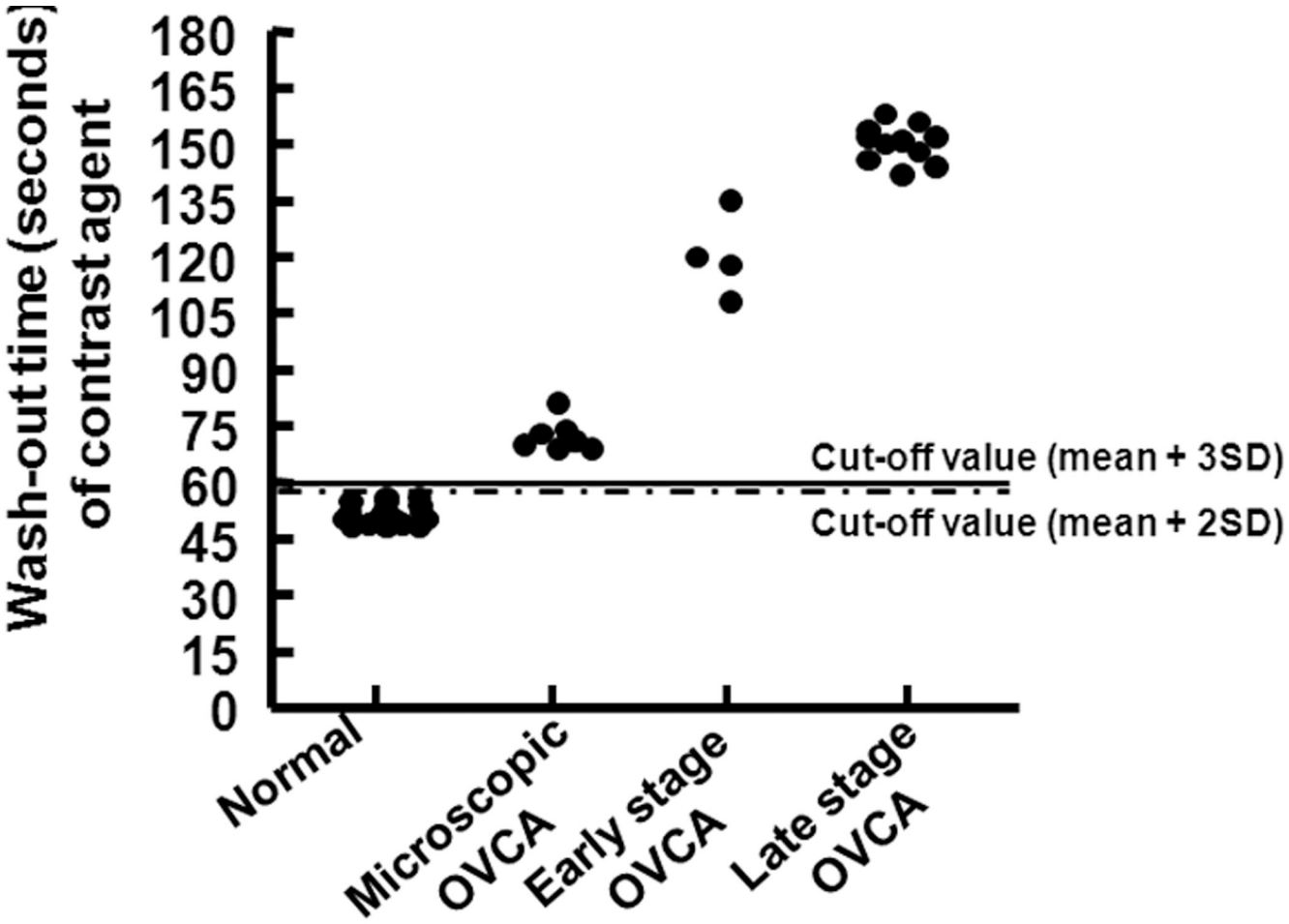

Figure 6.
Detection of ovarian tumor-associated neoangiogenesis by the wash-out time of the contrast agent. Other information is similar to the Figure 3. Cutoff lines (mean of wash-out time [seconds] of normal hens with 2 or 3 SDs) indicate the detectability of ovarian cancer (OVCA) by the wash-out time of the contrast agent.

Table 1

Changes in Doppler indices and the number of blood vessels in hen ovaries following the injection of Optison™.

Ovarian pathology	RI values		PI Values		Number of blood vessels	
	Before	After	Before	After	Before	After
Normal	0.68 ± 0.05 (0.60–0.80)	0.56 ± 0.05 (0.49–0.74)	1.05 ± 0.21 (0.83–1.46)	0.80 ± 0.11 (0.68–1.12)	3.29 ± 1.04 (2.00–5.00)	6.17 ± 1.31 (4.00–9.00)
Microscopic OVCA	0.59 ± 0.04 (0.54–0.66)	0.47 ± 0.03 (0.43–0.53)	0.88 ± 0.10 (0.74–1.08)	0.65 ± 0.08 (0.58–0.78)	5.14 ± 0.90 (4.00–6.00)	13.71 ± 3.90 (7.00–18.00)
Early stage OVCA	0.43 ± 0.01 (0.42–0.44)	0.33 ± 0.04 (0.29–0.38)	0.56 ± 0.02 (0.54–0.58)	0.44 ± 0.07 (0.36–0.53)	8.50 ± 1.00 (7.00–9.00)	18.50 ± 5.20 (15–26)
Late stage OVCA	0.36 ± 0.04 (0.30–0.40)	0.25 ± 0.04 (0.18–0.32)	0.46 ± 0.07 (0.34–0.56)	0.33 ± 0.07 (0.22–0.41)	12.91 ± 2.43 (10.00–18)	24.09 ± 4.61 (20–32)

Table 2

Kinetics of contrast agent relative to stages of ovarian cancer in hens.

Ovarian pathology	Time of arrival of contrast agent (secs)	Time to reach peak intensity (secs)	Time of wash-out (secs)	Percentage of hens with OVCA detected by Time-of-Washout*	Area under the curve (AUC)	Number of hens with OVCA detected by AUC*
Normal	15 ± 0.82 (14–16)	21 ± 0.81 (20–22)	51 ± 2.44 (48–56)	Ref	5496.94 ± 1439.80	Ref
Microscopic OVCA	14± 1.21 (12–15)	20 ± 2.04 (17–22)	72 ± 4.24 (69–81)	100% (P<0.01)	15310.86 ± 2771.64	86% (P<0.05)
Early stage OVCA	14 ± 0.96 (13–15)	19 ± 1.29 (17–20)	120 ± 11.15 (108–135)	100% (P<0.01)	49404.00 ± 10957.71	100% (P<0.05)
Late stage OVCA	13 ± 1.12 (11–14)	18 ± 0.94 (17–19)	150 ± 4.94 (142–156)	100% (P<0.01)	80607.00± 15247.76	100% (P<0.05)

Ref = reference

*above the cut-off value (mean of normal ± 3SD) for Time-of-Washout and AUC.